Quasi-Continuous Mode Conversion of Lamb Waves in CFRP Plates Due to Inhomogeneity on Micro and Meso Scale

Mirko N. Neumann, Bianca Hennings, Rolf Lammering

7th European Workshop on Structural Health Monitoring
July 8-11, 2014. La Cité, Nantes, France

QUASI-CONTINUOUS MODE CONVERSION OF LAMB WAVES IN CFRP PLATES DUE TO INHOMOGENEITY ON MICRO AND MESO SCALE

Mirko N. Neumann[1], **Bianca Hennings**[1], **Rolf Lammering**[1]

[1] *Helmut-Schmidt-University / University of the Federal Armed Forces Hamburg*
Institute of Mechanics, Holstenhofweg 85, 22043 Hamburg, Germany

mirko.neumann@hsu-hh.de

ABSTRACT

The mode conversion of symmetric into antisymmetric Lamb waves in non-damaged CFRP plates caused by their inhomogeneity is discussed. Lamb waves in differently stacked CFRP plates are observed via scanning laser vibrometry. In addition to the dominating wave crests observed propagating through the plates, as predictable from a macro-mechanical point of view, different patterns of parallel lines occur. These are analyzed and classified into three effects: Mode conversion at micro scale (fibers) and a static bending-stretching coupling effect at meso scale (weave rovings), also causing mode conversion under additional conditions. To consolidate the findings, tensile tests are performed and observed with a 3D image correlation method and a volume FE model of a twill fabric woven layer is used for static as well as dynamic simulations. The numerical results and the experimental data show a good agreement.

KEYWORDS : *Lamb waves, mode conversion, micro scale, meso scale*

INTRODUCTION

Lamb waves ([1], [2–4]) are well-suited for the detection of damages in thin-walled structures ([4–9]). At any excitation frequency they occur in at least two fundamental modes, the symmetric (S_i) and antisymmetric (A_i) modes. Higher wave modes are not discussed here. One effect of Lamb wave interaction with structural discontinuities is *mode conversion*: The primary wave group of one mode excites secondary waves of another mode at a discontinuity. S_0 waves converting into A_0 waves at an obstacle are depicted in Figure 1, left. The effect is utilized to detect structural damages. In order distinguish between damages and natural discontinuities, the systematic mode conversion at fibers and weave rovings in CFRP plates is investigated in this paper. First intense research on the subject is documented in [10]. The paper at hand adds fundamental thoughts to the matter, aiming at deepening the understanding.

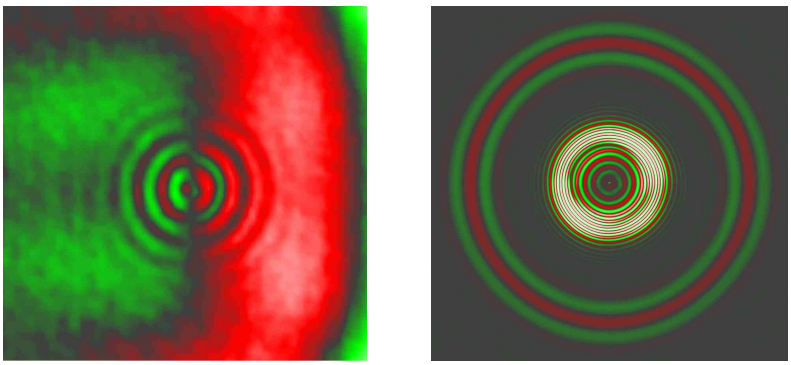

Figure 1 : Laser-vibrometric scans. Left: S_0 converting into A_0 mode at punctual obstacle (50kHz burst excitation in 1mm steel plate). Right: Burst-excited Lamb waves in 1mm aluminium plate at 100kHz.

The observation of different relevant effects via scanning laser vibrometry is presented. Parts of the results are identified to be caused by a static, position- and direction-dependent coupling effect between in-plane strain and bending via tensile tests. A finite element volume model is used to simulate both static loading and Lamb wave propagation in a realistically modeled woven CFRP structure. Simulations of wave propagation in a simplified two-dimensional model are used to show a frequency-influence on the occurrence of mode conversion.

1. LASER-VIBROMETRIC OBSERVATION OF MODE CONVERSION

A common technique for experimental Lamb wave observation is scanning laser vibrometry [11, 12]. Here, 1D-vibrometry is used, quantitative errors of the scanning data (see [13, 14]) occurring contrary to 3D-vibrometry, are neglected. As a simple example, Lamb waves propagating in circular wave crests in a homogeneous, isotropic plate, are depicted in Figure 1, right. The waves are excited through a piezoelectric ceramic disc glued to one surface. A two-period sine burst voltage is applied with the desired frequency. For better frequency selectivity, a von-Hann-window is used.

1.1 CFRP plates consisting of unidirectional layers

Now, anisotropic plates are under consideration. Since antisymmetric Lamb wave behavior depends on flexural, and symmetric on axial plate stiffness, the wave crests of the two fundamental modes show a great difference to the isotropic case and also to one another, cf. the velocity fields in a cross-ply laminate built up from four unidirectional laminae UD255g/m^2 $[0°/90°]_S$ in Figure 2.

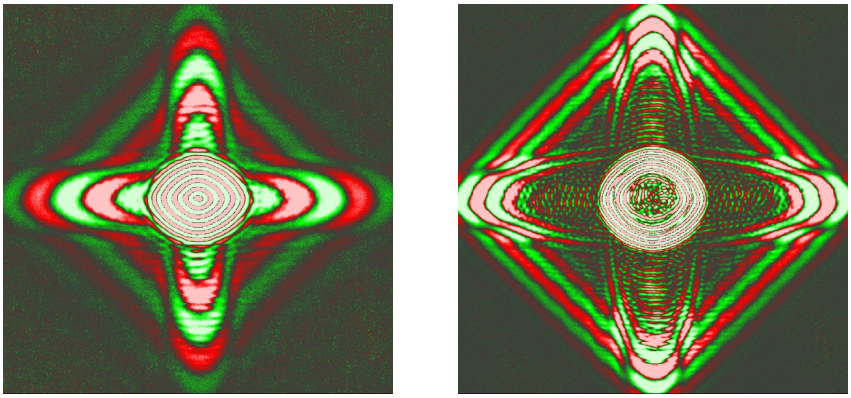

Figure 2 : Lamb waves in cross-ply built from UD layers. Left: 50kHz, right: 100kHz.

In both plots, waves are visible within, respectively, behind the primary S_0 group. These are identified as secondary A_0 Lamb waves due to their wavelength, as a result from mode conversion of S_0 into A_0, because they exist before the A_0 group has reached the concerned areas due to its slowness.

Since the laminate exclusively consists of UD layers and the effect takes place only parallel to fiber directions, the mode conversion is stated to be generated at the scale of the fiber diameter, i.e. at microscale. The effect occurs at any tested frequency. For extended information about this phenomenon, see [15], where the results of numerical investigations are presented.

1.2 CFRP plates consisting of woven layers

CFRP laminates can not only be built up from unidirectional laminae but also from woven layers or combinations of both. With each method, the same macro-mechanical properties can be achieved, i.e. equal ABD-matrices, [16, 17], may describe different set-ups. So, Figure 3 shows respective velocity

fields in a cross-ply laminate built up from six woven *twill fabric 'Köper 2/2'* layers 3k$[6*0°]$.

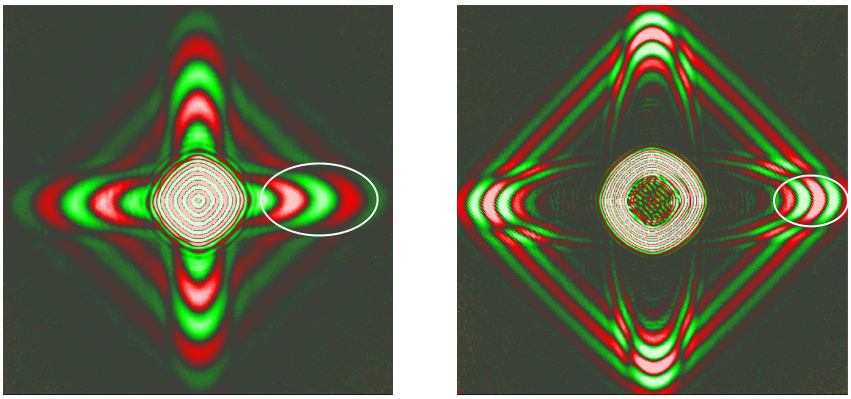

Figure 3 : Lamb waves in cross-ply built from twill fabric layers. Left: 50kHz, right: 100kHz.

In addition to the mode conversion parallel to the main axes (right picture only), a 45° pattern is visible within the S_0 group. As seen from the right picture, this effect dies away after S_0 passes. The distance between two lines of the pattern matches the weave structure of the plate surface. It is hence assumed to be a static effect, coupling axial and local bending deformation.

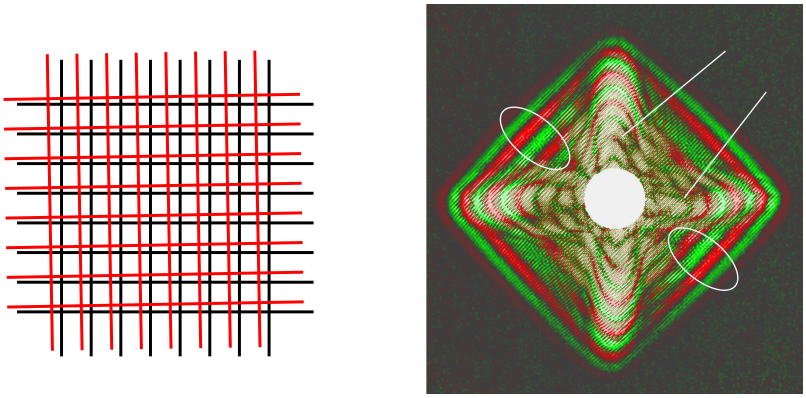

Figure 4 : Left: Geometric shift between layers of a multi-layered cross-ply, right: Lamb waves in single-layer twill fabric plate at 100kHz.

In single layer woven plates, the coupling effect emerges with a greater magnitude due to no compensation effects due to added stiffness, nor any in-plane shift between different layers (see Figure 4, left). Figure 4 (right) depicts Lamb waves in a single layer twill fabric plate. It becomes visible, that no coupling occurs in the encircled areas. Also, straight lines with angles varying from the 45° direction emerge. These additional circumstances are discussed later within the paper.

2. Experimental tensile tests

The assumed coupling effect is investigated via quasi-static tensile testing of single layer twill fabric plates, where the phenomenon appears strongest. A standard tensile testing machine is used to load specimens of 25mm width. The displacement observation on the surface is performed with a digital "4D" image correlation system Q-400 from Dantec Dynamics.

The observed surface is speckled with a statistic pattern of high contrast to allow tracking of local deformation. Two digital cameras record images at every load step, each containing two-dimensional

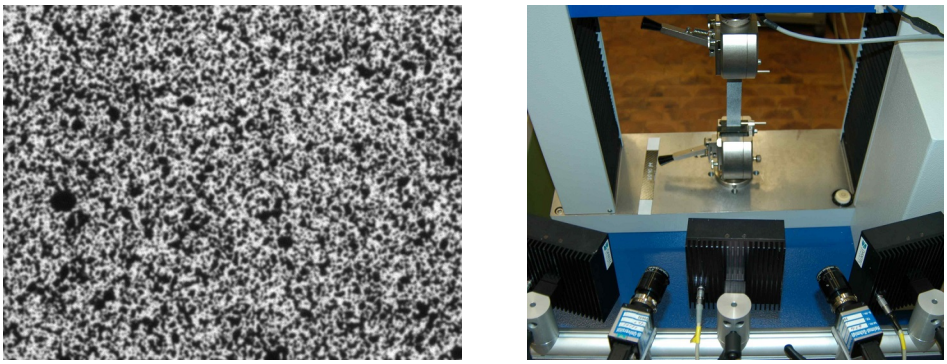

Figure 5 : Left: Surface prepared for camera observation. Right: Camera set-up with clamped specimen in testing machine.

information of the displacement field from different viewing directions. From this data, the quantified displacements are successively computed.

The technique can be used with a single camera in order to obtain 2D in-plane information. With two cameras, the 3D spatial data is obtained from an overdetermined (4D) system, as used in this case. The specimen is loaded continuously, the images are recorded as a movie at a specified framerate. The experimental set-up is shown in Figure 5.

After tensile loading of the specimens, the 45° pattern shows up, proving the static nature of this effect. Figure 6 (left) shows the results of a specimen at 0°-orientation. The behavior is the same for the 90° direction (no picture), however, *no coupling is observed for the ±45° directions* (no picture).

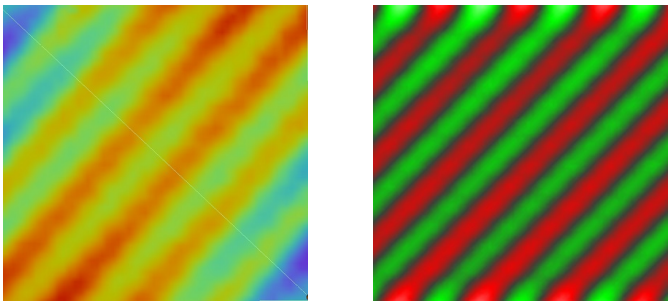

Figure 6 : Out-of-plane displacement in tensile loading of 0° specimen. Left: experiment; right: FE simulation.

3. FINITE ELEMENT MODELING

The position- and direction-dependent coupling has to be modeled at the mesoscale, because the common method of homogenization yields only the macromechnical description of the model. The individual properties of the fiber- and matrix material are two-dimensionally accounted for in a model for UD-layers in this research group, see [15].

Woven layers require a three-dimensional model which cannot be achieved with standard computer equipment at fiber-/microscale. However, woven layers have another scale of inhomogeneity. Each roving can be thought of as a transverse-isotropic thread. Following this idea, the model size is reduced and is still at the mesocale.

Figure 7 (top) depicts the micrograph of a cross-section of a CFRP twill fabric layer. The single rovings are clearly visible as individual entities. Due to the woven structure, the cross-section of a single roving is twisted from one thread to another. By use of hexagonally shaped areas this twist can be discretized, see Figure 7, bottom.

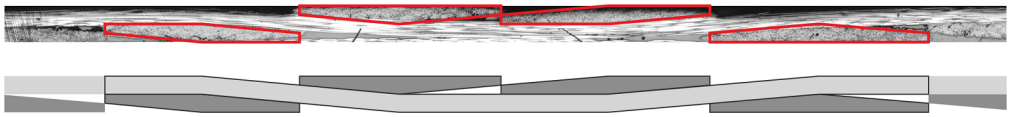

Figure 7 : Micrograph of a cross-section of a twill fabric layer (top) and zonally homogenized model (bottom).

For a three-dimensional model of the twill woven structure, the hexagonal shape of the rovings cross sections is the simplest possible option for the volumetric bodies not to penetrate each other. All bodies consist of a wireframe of straight lines, leading to some of the boundary areas being non-planar patches.

Like in the real structure, volumes exist which only consist of pure matrix material without fibers ('resin pockets'), although in the model, their percentage (25%) is slightly higher due to the straight-lined wireframe, where on the contrary the rovings are curved in reality. The geometric model is shown in Figure 8. The spaces filled with matrix material are blinded out for better visualization. The shape of these spaces require to use tetrahedral finite elements.

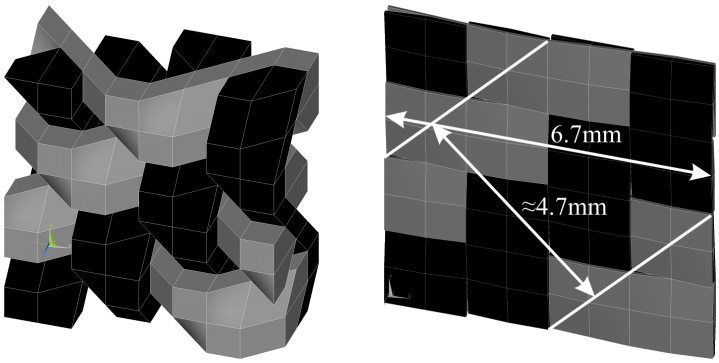

Figure 8 : Representative volume element of twill fabric plates. Left: scaled to unit lengths, right: proportional scaling (6.7mm $\times$ 6.7mm).

The advantage of the precise model of the real structure is paid by a high computational effort: One representative volume element has 2882 nodes for a 'Köper 2/2' twill fabric layer '3k' (3000 fibers per roving) and covers an area of 6.7mm $\times$ 6.7mm.

4. Numerical tensile tests

Tensile tests are simulated for comparison with the experiments presented in Section 2. Figure 6 (right) depicts the out-of-plane displacements obtained from a numerical tensile test in 0°-direction. The experimental result in Figure 6 (left) is confirmed. Again the coupling effect does not arise for the $\pm$45°-direction (no picture). In Table 1, the macroscopic Young's moduli of the discussed examples are compared. The simulation results give an acceptable match with the real structure.

Table 1 : Comparison of Young's moduli obtained from experimental and simulated tensile tests.

Angle	$\mathbf{E}_{\text{exp}}$/GPa	$\mathbf{E}_{\text{FEM}}$/GPa
0°	51	46
90°	46	45
45°	14	14
−45°	12	14

After building a model containing only the rovings in x-direction, the sign of the local out-of-plane deformation will be constant for any load direction, but the absolute value becomes minimal for 90° (no picture). Building a model exclusively from y-rovings, the opposite sign occurs for any load direction, with a minimum value at 0° (no picture).

Performing the experiment with the original model (x- and y-rovings considered), the sign of each roving direction dominates for their respective tension directions, and minima (with change of sign) occur at the ±45°-directions, cf. Figure 9.

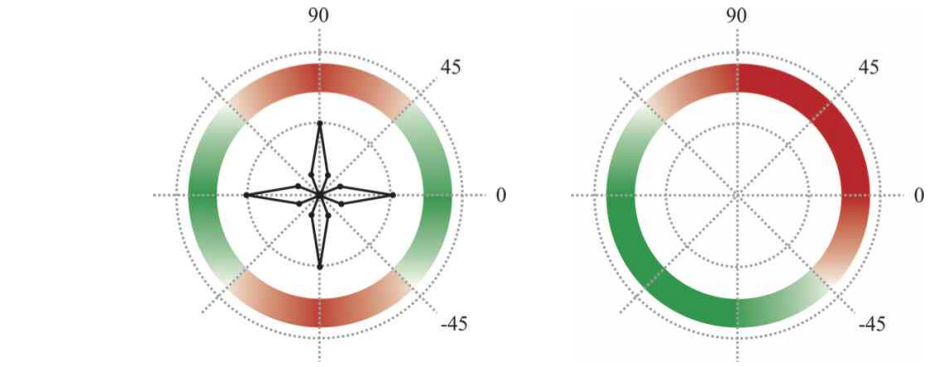

Figure 9 : Left: Value and signum of out-of-plane coupling from tensile tests (with respect to specimen angle). Right: Polar signum distribution of coupling due to wave propagation.

5. LAMB WAVE SIMULATION

In order to limit the computational costs only single layer plates are considered in the numerical analysis. The necessarily very flat element shapes have a negative influence on the precision. Nevertheless, pressure (S_0) waves agree well with analytic solutions, however, the antisymmetric modes show an error in wavelength. For the sake of brevity, the basic investigations on this are not discussed here. For Lamb wave simulation, the numerical results are in good agreement with the experiment again, cf. surface plots at 100kHz in Figure 10. At the given frequency, the A_0 mode wavelength (center of surface plot) clearly differs from the diagonal pattern superimposing the S_0 mode due to coupling, making it possible to distinguish both.

In contrast to quasi-static tensile tests, the polar sign distribution in one tension phase zone of the propagating S_0 wave has only two changes at $-45°$ and 135°, see Figure 9, right. The reason for

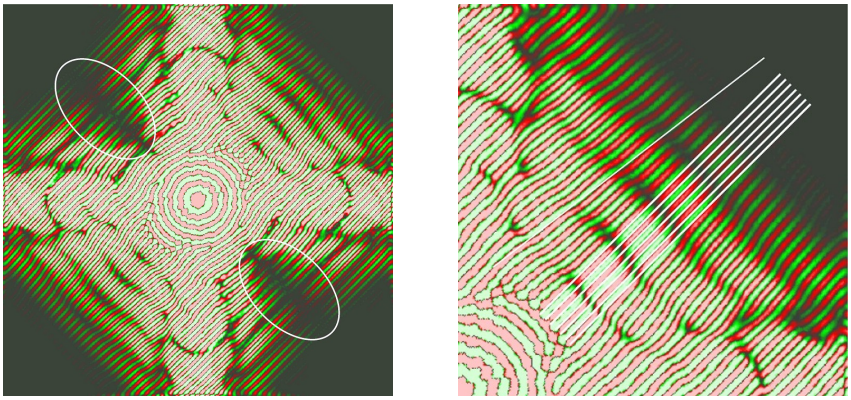

Figure 10 : Simulation results: Lamb waves at 100kHz in a 268mm × 268mm × 0.28mm single layer twill fabric plate. Right: Detailed view of upper right quadrant. White lines for the identification of non-45° oblique lines.

this circumstance is currently being investigated with respect to the macromechanical shear-coupling behavior of the orthotropic plate properties. Figure 10 (right) shows the formerly mentioned oblique lines deviating from the 45°-angle which are identified as sign changes between tension and pressure phase zones of the S_0 mode. This is difficult to discover from experimental data, however, the numerical results allow a more precise insight here.

6. FREQUENCY DEPENDENCE OF COUPLING-INDUCED MODE CONVERSION

Lamb wave measurements in plates from unidirectional layers show mode conversion at any tested frequency. This is due to the random distribution of fibers in the matrix material, cf. [15]. At mesoscale, the weave rovings follow a very regular periodic pattern in relation to their geometric dimensions. Basic investigations on mode conversion at interchanging coupling behavior between stretching and bending are performed with a simplified 2D-model, confirming experimental results. For sake of brevity, only the most important results are discussed here.

In such regular coupling structures, mode conversion does not occur for A_0 wavelengths namely larger than a 'coupling element' (see Figures 3 and 8), i.e. at the corresponding low frequencies. With increasing frequency and smaller A_0 wavelengths, in the range of the coupling element or smaller, mode conversion occurs at every coupling element, quasi continuously over the whole structure.

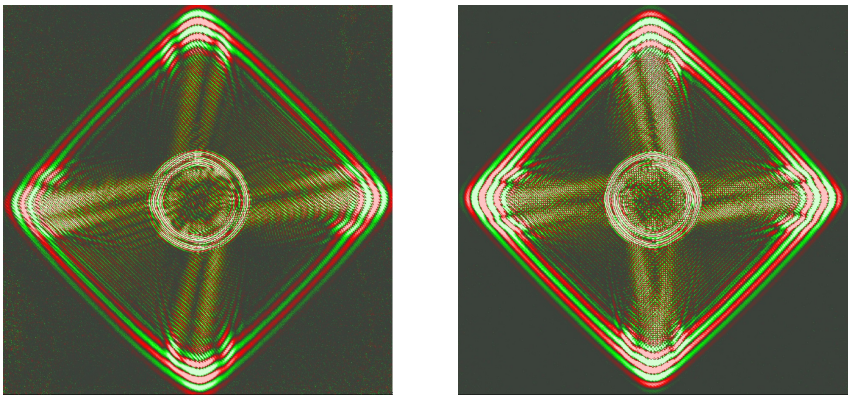

Figure 11 : Lamb waves at 200kHz in cross plys 3k$[6*0°]$ (left) and 3k$[0/90/0/90/0/90]$ (right)

Figure 11, left, depicts the Lamb wave field in a 3k$[6*0°]$ twill fabric plate of six layers, all with a rotation angle of 0°. The excitation frequency is 200kHz. At this frequency, the A_0 wavelength is about 5mm, matching the dimension of the coupling effect, which is $6.7\text{mm}/\sqrt{2} \approx 4.7\text{mm}$. Between the primary S_0 and A_0 wave groups, secondary A_0 Lamb waves are visible, excited by mode conversion of the S_0 mode. In Figure 11, right, the experiment is repeated with a plate with the stacking sequence 3k$[0/90/0/90/0/90]$. Here, the coupling effect exists for both diagonal ($\pm 45°$) directions. Mode conversion occurs again, accordingly in both directions in the different layers.

CONCLUSION

Within this paper, Lamb wave propagation in CFRP plates is under investigation. After transient burst excitation and separation of the primary A_0 and S_0 Lamb wave groups, a secondary A_0 mode is identified, originating from mode conversion of the primary S_0 group, although the plate specimens are assumed to be free of structural damages.

The occurrence of mode conversion in intact plates made of unidirectional prepreg layers leads to the assumption, that the effect originates at the microscale, i.e. the micromechanics of fiber-matrix interaction. This has been confirmed in [15]. For UD layers, the occurrence of the effect has proved to be frequency-independent.

In the case of CFRP laminates built of twill fabric layers, another phenomenon arises, which turns out to be a static coupling effect between stretching and bending of the plate. The effect is locally and directionally varyring at the mesoscopic scale. It is induced by the inner structure of twill weave fabric. The assumptions are confirmed via tensile tests with a digital image correlation measurement technique. A precise geometric finite element model of the weave structure is used to confirm static as well as dynamic experimental results and explains side effects observed in the experiments. Through additional FE simulations, the frequency dependency of mode conversion originating from the coupling effect is determined and experimentally confirmed.

By these investigations findings in [10] are confirmed and broadened. Research at issue deals with a quantitative study on damping of Lamb waves due to mode conversion and interference with signals of punctually applied sensors.

ACKNOWLEDGEMENT

The financial support of the Deutsche Forschungsgemeinschaft is gratefully acknowledged.

REFERENCES

[1] H. Lamb. On waves in an elastic plate. *Proc. Royal Soc. of London Series A*, XCIII:114–128, 1914.

[2] K. F. Graff. *Wave motion in elastic solids*. Dover Publications, New York, 1991.

[3] J. L. Rose. *Ultrasonic waves in solid media*. Cambridge Univ. Press, Cambridge, 2004.

[4] V. Giurgiutiu. *Structural health monitoring with piezoelectric wafer active sensors*. Academic Press/Elsevier, Amsterdam, 2008.

[5] W. J. Staszewski, B. C. Lee, L. Mallet, and F. Scarpa. Structural health monitoring using scanning laser vibrometry: I. Lamb wave sensing. *Smart Materials and Structures*, 13:251–260, 2004.

[6] L. Mallet, B. C. Lee, W. J. Staszewski, and F. Scarpa. Structural health monitoring using scanning laser vibrometry: II. Lamb waves for damage detection. *Smart Materials and Structures*, 13:261–269, 2004.

[7] W. H. Leong, W. J. Staszewski, B. C. Lee, and F. Scarpa. Structural health monitoring using scanning laser vibrometry: III. Lamb waves for fatigue crack detection. *Smart Materials and Structures*, 14:1387–1395, 2005.

[8] W. J. Staszewski, B. C. Lee, and R. Traynor. Fatigue crack detection in metallic structures with Lamb waves and 3D laser vibrometry. *Measurement Science and Technology*, 18:727–739, 2007.

[9] R. Lammering and M. Neumann. Optical Measurement Techniques for Use of Defect Detection in Thin Walled Structures. In Fabio Casciati and Michele Giordano, editors, *Proceedings of the Fifth European Workshop on Structural Health Monitoring 2010*, 2010.

[10] C. Willberg, S. Koch, G. Mook, J. Pohl, and U. Gabbert. Continuous mode conversion of Lamb waves in CFRP plates. *Smart Materials and Structures*, (21), 2012.

[11] A. Donges and R. Noll. *Lasermeßtechnik: Grundlagen und Anwendungen*, volume 4 of *Technische Physik*. Hüthig, Heidelberg, 1993.

[12] Polytec GmbH. *Polytec Scanning Vibrometer Theory Manual*. Self-publishing, Waldbronn, 2010.

[13] M. N. Neumann and R. Lammering. Error Analysis in Laser Vibrometer Measurements of Lamb Waves. In DGZfP e.V., editor, *Proceedings of the Sixth European Workshop on Structural Health Monitoring (EWSHM 2012)*, volume 1, pages 729–736, 2012.

[14] M. N. Neumann, B. Hennings, and R. Lammering. Identification and Avoidance of Systematic Measurement Errors in Lamb Wave Observation With One-Dimensional Scanning Laser Vibrometry. *Strain*, 49(2):95–101, 2013.

[15] B. Hennings, M. N. Neumann, and R. Lammering. Continuous Mode Conversion of Lamb Waves in Carbon Fibre Composite Plates - Occurrence and Modelling. In F.-K. Chang, editor, *Proc. 9th International Workshop on Structural Health Monitoring*, Lancaster, PA, USA, 2013. DEStech Publ., Inc.

[16] R. M. Jones. *Mechanics of Composite Materials*. Scripta Book Company, Washington D.C USA, 1975.

[17] J. N. Reddy. *Mechanics of laminated composite plates and shells: Theory and analysis*. CRC Press, Boca Raton and Fla, 2 edition, 2004.